Dynamical Downscaling of Wind Speed in Complex Terrain Prone To Bora-Type Flows

KRISTIAN HORVATH, ALICA BAJIĆ, AND STJEPAN IVATEK-ŠAHDAN

Meteorological and Hydrological Service, Zagreb, Croatia

(Manuscript received 30 August 2010, in final form 18 March 2011)

ABSTRACT

The results of numerically modeled wind speed climate, a primary component of wind energy resource assessment in the complex terrain of Croatia, are given. For that purpose, dynamical downscaling of 10 yr (1992–2001) of the 40-yr ECMWF Re-Analysis (ERA-40) was performed to 8-km horizontal grid spacing with the use of a spectral, prognostic full-physics model Aire Limitée Adaptation Dynamique Développement International (ALADIN; the ''ALHR'' version). Then modeled data with a 60-min frequency were refined to 2-km horizontal grid spacing with a simplified and cost-effective model version, the so-called dynamical adaptation (DADA). The statistical verification of ERA-40-, ALHR-, and DADA-modeled wind speed on the basis of data from measurement stations representing different regions of Croatia suggests that downscaling was successful and that model accuracy generally improves as horizontal resolution is increased. The areas of the highest mean wind speeds correspond well to locations of frequent and strong bora flow as well as to the prominent mountain peaks. The best results are achieved with DADA and contain bias of 1% of the mean wind speed for eastern Croatia while reaching 10% for complex coastal terrain, mainly because of underestimation of the strongest winds. Root-mean-square errors for DADA are significantly smaller for flat terrain than for complex terrain, with relative values close to 12% of the mean wind speed regardless of the station location. Spectral analyses suggest that the shape of the kinetic energy spectra generally relaxes from k^{-3} at the upper troposphere to the shape of orographic spectra near the surface and shows no seasonal variability. Apart from the buildup of energy on smaller scales of motions, it is shown that mesoscale simulations contain a considerable amount of energy related to near-surface and mostly divergent meso-β-scale (20–200 km) motions. Spectral decomposition of measured and modeled data in temporal space indicates a reasonable performance of all model datasets in simulating the primary maximum of spectral power related to synoptic and larger-than-diurnal mesoscale motions, with somewhat increased accuracy of mesoscale model data. The primary improvement of dynamical adaptation was achieved for cross-mountain winds, whereas mixed results were found for along-mountain wind directions. Secondary diurnal and tertiary semidiurnal maxima are significantly better simulated with the mesoscale model for coastal stations but are somewhat more erroneous for the continental station. The mesoscale model data underestimate the spectral power of motions with less-than-semidiurnal periods.

1. Introduction

Climatological wind behavior is the crucial factor for establishing the meteorological basis for the assessment of wind energy resources. Typically, global reanalysis data (which are available on ~100-km horizontal grid spacing or more) are not sufficiently accurate for assessment of the wind climate in the planetary boundary layer, especially over complex terrain. Therefore, to attain both spatial and temporal representativeness, these data must be downscaled over the target area over a substantially long time period. A common method for estimation of wind climate in complex terrain (especially in areas of scarce or nonexistent high-quality measurements) is dynamical downscaling with the use of mesoscale numerical weather prediction models. The spatial and temporal refinement of wind climate depends on the mesoscale model resolution, which should be chosen using knowledge of the spatial and temporal scales of the atmospheric phenomena occurring in the target area.

In general, dynamical downscaling is expected to introduce additional (smaller) spatial and temporal scales,

Corresponding author address: Dr. Sc. Kristian Horvath, Grič 3, 10000 Zagreb, Croatia.
E-mail: kristian.horvath@cirus.dhz.hr

DOI: 10.1175/2011JAMC2638.1

resulting in a more adequate reproduction of mesoscale wind systems. These systems are most often either a result of terrain and surface inhomogeneities (such as land–sea breezes, katabatic winds, and valley winds) or of interaction between terrain and the large-scale flow (such as downslope windstorms, gravity waves, gap flows, and wakes). It is the coastal mountainous region of the eastern Adriatic coast (the area with the greatest wind resources in Croatia) that is frequently subject to strong wind systems that are embedded in a range of intense and interrelated subsynoptic phenomena within the region (e.g., Horvath et al. 2008). In particular, the gusty and severe downslope windstorm known as bora (e.g., Smith 1985, 1987; Klemp and Durran 1987), with hurricane-scale gusts that can reach 70 m s^{-1}, is especially important for wind energy applications. Indeed, the relevance of this phenomenon[1] and considerable research related to the Croatian bora [see review by Grisogono and Belušić (2009)] suggest that the eastern Adriatic coast might be an excellent target area for evaluation of the performance of mesoscale models for complex terrain prone to downslope windstorms.

In addition to the bora (which accounts for the largest portion of wind energy potential in the target region), another wind system of importance that blows along the eastern Adriatic coast is the southeasterly "jugo"[2] wind. The nature of bora and jugo winds, which are strongly determined by the orographic pressure perturbation, suggests that the ability of mesoscale models to simulate nonlinear flows and flows over mountains under different regimes of background flow[3] is an important and desired feature relevant for the success of modeling the representative wind climate or estimating regional wind resources.

Because the available wind power potential is proportional to the cube of the wind speed (e.g., Troen and Petersen 1989), the precision requirements for a wind speed "climatology" for energy assessment are higher than for most other purposes. In particular, this holds for stronger wind speeds because small relative errors (especially near the wind turbine cut-out wind speed of 25 m s^{-1}) can have profound effects on the assessment of available wind power. Therefore, in addition to analysis and verification of the modeled wind speeds, meaningful analyses of both potential (including all wind speeds) and actual (including only the range of wind speeds at which wind turbines operate) wind resources might be performed using wind power density[4] instead. Although we do consider wind resource assessment as a primary application, we choose to evaluate the accuracy of dynamically downscaled wind speed since 1) dynamically downscaled wind speed climate has other applications than wind energy and 2) for actual wind resource assessment a number of other specific technical issues need to be taken into account.

Despite the widespread use of mesoscale models for analysis and assessment of winds and wind climate properties, verification of their performance is a challenging issue that often does not follow a unified approach. Statistical verification that uses basic verification parameters (systematic error, root-mean-square error, etc.) seems not to be sufficient for the purpose. This is because small errors in time or space of the otherwise well-simulated particular phenomena can profoundly change the verification results (e.g., Mass et al. 2002). Therefore, it is often favorable to utilize a spectral analysis as a complimentary verification method so as to provide a scale-dependent measure of model performance as well as more detailed insight into the ability of the model to simulate local wind climates. For example, the evaluation of power spectra from measured and modeled time series facilitates the evaluation of model performance on different temporal scales (e.g., synoptic, mesoscale, diurnal, semidiurnal, and subsemidiurnal) regardless of the potential phase errors. On the other hand, the success of models in simulating the proper shape of the kinetic energy spectrum in a spatial domain can serve as a prime tool for qualitative model evaluations.

The primary goal of this paper is to present the results of the performed dynamical downscaling for a 10-year period with the use of the Aire Limitée Adaptation Dynamique Développement International (ALADIN) mesoscale model. A second goal is to assess the ability of the mesoscale model to reproduce the relevant wind speed climate in the complex terrain of Croatia as a basis for wind energy assessment. This is achieved by means of statistical and spectral verification at selected stations. Furthermore, spatial spectra of the kinetic energy, vorticity, and divergence are used to study the ability of the ALADIN model to reproduce universally observed spectra in the free troposphere and also to

[1] The areas characterized by bora-type flows include, but are not limited to, southern California, the Rocky Mountains, the Andes, and areas of Italy, Slovenia, Austria, Iceland, New Zealand, Sumatra, Japan, Indonesia, Kurdistan, and Russia.

[2] Jugo is a local name for a southeasterly wind that occurs over the wider region of the Adriatic Sea. It belongs to the family of southwesterly Mediterranean sirocco winds that are channeled in the southeasterly direction by the Dinaric Alps (Jurčec et al. 1996).

[3] Background flow is the flow impinging on the mountain that at first approximation (together with mountain height and shape) determines the leeside response. Its most important properties are its cross-mountain wind speed component and its (moist) static stability.

[4] Wind power density (W m^{-2}) is defined as $P = 0.5\rho V^3$, where ρ is air density and V is wind speed.

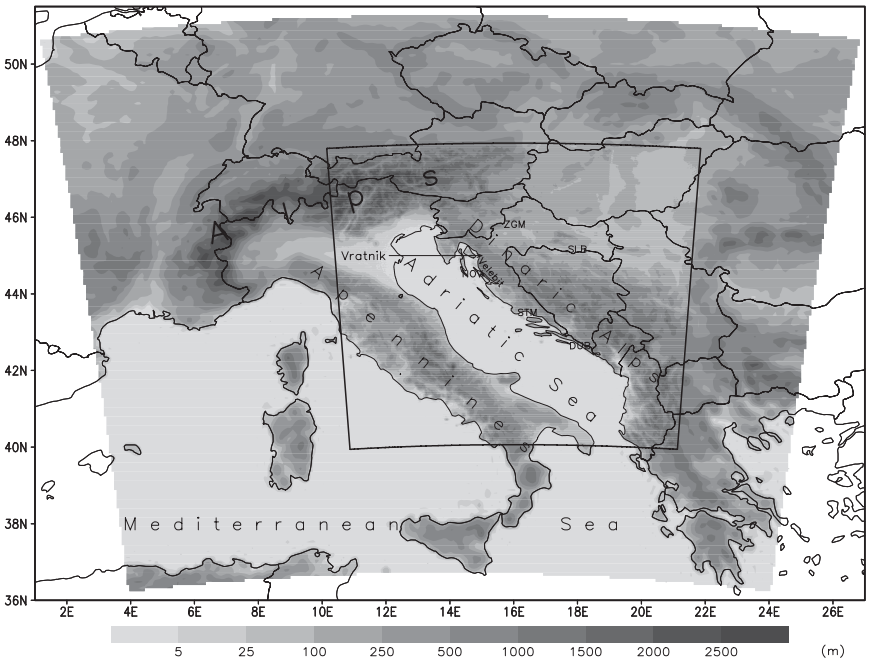

FIG. 1. The integration domain of the ALADIN model at 8-km (larger shaded area) and 2-km (inner shaded area) grid spacing with the associated digital elevation terrain models as well as geographic features and measurement stations referred to in the text.

study the mesoscale spectra at near-surface levels that are relevant to wind energy applications.

The paper is organized as follows. The method is described in section 2. The results of the dynamical downscaling are presented in section 3, and statistical and spectral analyses and verification are presented in section 4. Conclusions are given in section 5.

2. Method

Dynamical downscaling was performed with the ALADIN mesoscale model (Bubnova et al. 1995). ALADIN is used for everyday numerical weather prediction (typically at 4–10-km grid spacing) in over a dozen countries (http://www.cnrm.meteo.fr/aladin/). ALADIN is a primitive equation spectral model with a hybrid η coordinate (Simmons and Burridge 1981) and a two-time-level, semi-implicit semi-Lagrangian scheme. Model fields in spectral space are obtained by double Fourier transform, and the biperiodicity is satisfied by introducing the extension zone (Machenhauer and Haugen 1987). The Davies (1976) relaxation scheme is used for coupling with the driving model. Physical parameterizations include vertical diffusion (Louis et al. 1982) and shallow convection (Geleyn 1987). Kessler-type parameterization is used to account for resolved precipitation (Kessler 1969), and deep convection is modeled with a modified Kuo scheme (Geleyn et al. 1982). Radiation is described following Geleyn and Hollingsworth (1979) and Ritter and Geleyn (1992). A two-layer soil scheme (Giard and Bazile 2000) is used to simulate vertical transport of soil moisture and heat.

The model is run in a hydrostatic mode with 37 vertical levels (the lowest model level is at 17 m) and 8-km horizontal grid spacing. The model domain is shown in Fig. 1. Initial and boundary conditions were provided by the global reanalysis of the 40-yr European Centre for Medium-Range Weather Forecasts (ECMWF) Re-Analysis (ERA-40; Kållberg et al. 2004), which is available at 125-km grid spacing with a 6-hourly frequency. Following the methods of Beck et al. (2004) and Žagar et al. (2006), a direct nesting strategy was implemented. These authors showed that the dynamical downscaling of ERA-40 data with the ALADIN model to ~10-km grid spacing is equally accurate whether or not an intermediate domain is used. Although there is no doubt that in some individual cases and events this nesting ratio would be excessive (e.g., because of very large spin-off times), it appears that for wind climate estimates the proposed approach is sufficient. Prior to integration, the data were interpolated in space and were filtered using a digital filter initialization procedure (Lynch and Huang 1994). The model was initialized daily at 1200 UTC and was run for 36 h; the output data were archived with 60-min frequency. Because of the large grid ratio, a 12-hourly spinup time was provided to allow sufficient time for the buildup of mesoscale energy in

the model (Žagar et al. 2006). This version of the ALADIN model setup is referred to as ALHR.

Upon integration, the 24-hourly period (beginning with the 12-hourly forecast range) was refined to a 2-km model grid on a subdomain (Fig. 1) with so-called dynamical adaptation (Žagar and Rakovec 1999). Dynamical adaptation (DADA) is a cost-effective method of dynamically adjusting near-surface winds from low-resolution to a finer-resolution orography with a simplified mesoscale-model version that is used operationally in Croatia (Ivatek-Šahdan and Tudor 2004). The main simplifications include a reduced number of vertical levels above the planetary boundary layer and withheld parameterizations of moist processes and the effects of radiation. Several dozens of time steps are usually required to reach the quasi-stationary state of dynamical adjustment that is achieved with the use of time-invariant lateral boundary conditions from the driver model. The procedure typically results in dynamically adjusted near-surface winds considerably faster (close to 70 times in the Croatian model chain) than does full model integration at the same grid spacing. As described by Žagar and Rakovec (1999), dynamical adaptation will typically be more effective and accurate when pressure gradients are stronger, because 1) dynamical forcing is of primary importance and all other forcing (such as radiative or that due to moist processes) is of secondary importance and 2) for stronger pressure gradients the adaptation is achieved in a reasonably short time interval (less than 30 min). These conditions suit the wind resource modeling in terrain prone to strong bora flows well. In some situations, dynamical adaptation is not expected to bring an added value; these include quick passages of cold fronts (due to nonstationarity and the role of moisture), as well as valley inversions and thermal circulations that are unresolved by the driver model (because in the setup of dynamical adaptation the radiation scheme is switched off) and other errors in the input data. A more comprehensive description of dynamical adaptation can be found in Žagar and Rakovec (1999); here we briefly describe the model setup. The simplified model version was ran for 30 time steps (of 60 s each) with the same number of vertical levels below 1000 m (8) and a reduced number of vertical levels above (7 instead of 29). All physical parameterizations were withheld except for the parameterization of vertical diffusion.

3. Results

a. Spatial distribution of mean wind speed

Mean 10-yearly wind speed at 10 m AGL over the downscaling period (1992–2001) is shown in Fig. 2. The main feature of the spatial distribution is considerably higher wind speed in the wider coastal area and hinterlands than in the continental part of Croatia. The highest mean wind speed over the land is simulated over the eastern slopes of Velebit Mountain (including the proximate areas above the sea) as well as over the higher ridges and mountaintops. Although mountaintops are often regions of enhanced wind resource because of their altitude, the high-wind-resource area over the western slopes of Velebit Mountain results primarily from the climatologically high frequency of bora (Yoshino 1976; Bajić 1989; Poje 1992; Cavaleri et al. 1997). The channeling of the northeasterly background flow during bora events through the Vratnik Pass (e.g., Makjanić 1976; Göhm et al. 2008) contributes to the local enhancement of wind speed. This leeside maximum extends offshore and reaches the outermost islands, acquiring a spatial distribution that resembles the hydraulic solutions for bora flows (e.g., Smith 1985) and reaches the absolute maximum of mean 10-m wind speed that is close to 6.5 m s^{-1}. On the other hand, the spatial confinement of the leeside maxima to the vicinity of the western slopes of southern Velebit indicates the preference for the other mechanism applicable to strong bora flows, which is related to upstream blocking and gravity wave breaking (e.g., Klemp and Durran 1987). The nonexistence of such a maximum over the western slopes of the southern Dinaric Alps is primarily related to the lower frequency of the favorable synoptic setting required for the onset of bora. In addition, the results could be influenced by the lower predictability and weaker model performance over the middle and southern Adriatic and associated underestimation of strong bora flows (Horvath et al. 2009). The regions with the weakest 10-yearly mean wind speeds are primarily some of the lowland areas of continental Croatia.

These results suggest that bora downslope windstorms are extremely important for wind energy utilization in the coastal area of Croatia. Because of the gusty character of bora and the extreme turbulence that may result in turbulent kinetic energy of over 30 J kg^{-1} (Belušić and Klaić 2006), however, future estimates of wind resources in the region must include the net effects of bora turbulence. Therefore, higher-resolution modeling and more insight into the properties of bora turbulence seem to be the remaining challenges, not only of scientific advancements in the broad area of bora-type flows, but also of relevant wind energy applications in complex terrain.

b. Statistical verification

Statistical model verification was performed for ERA-40, ALHR, and DADA datasets using measured wind speed data from 2001 from four meteorological stations (see Fig. 1) that represent the different climate regimes of Croatia. The station of Slavonski Brod (SLB) is representative

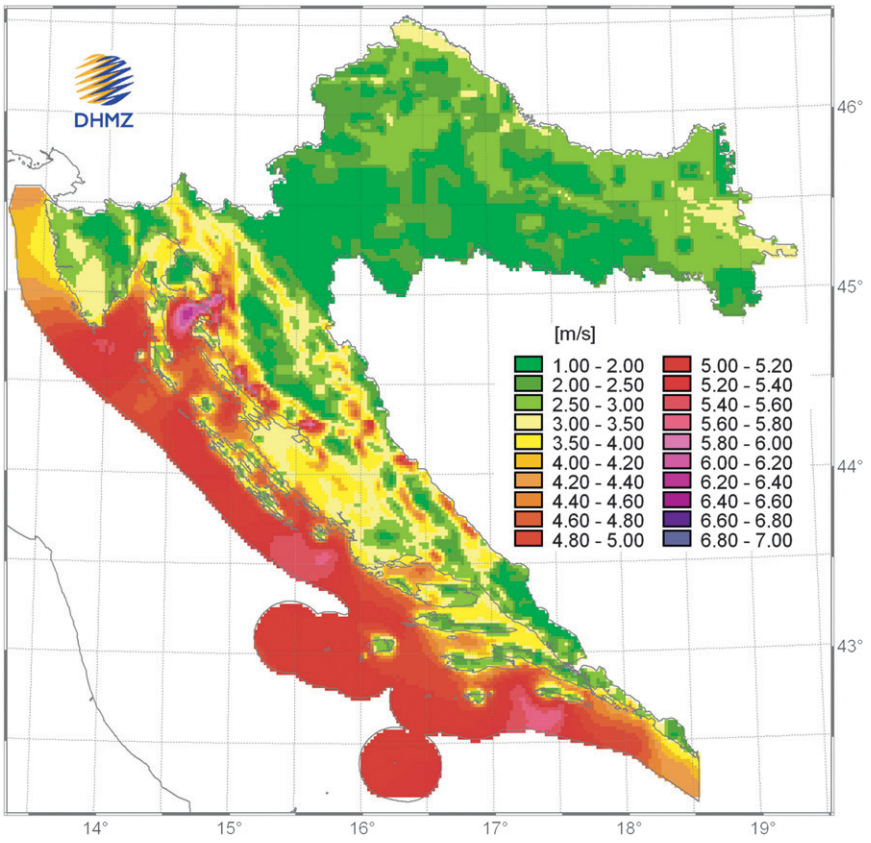

FIG. 2. The spatial distribution of 10-yearly mean wind speed (1992–2001) (m s^{-1}) at 10-m AGL as a direct model output of the dynamical adaptation at 2-km horizontal grid spacing.

of the moderate continental climate and wind climates found in flat and gently sloped terrain. Stations Novalja (NOV), Split Marjan (STM), and Dubrovnik (DUB) were selected for model verification of maritime climate (e.g., Zaninović et al. 2008) that is characterized by the proximity of the complex terrain of the Dinaric Alps. The model data were bilinearly interpolated to the station locations without any other postprocessing or corrections except for the use of similarity theory to deduce the 10-m winds. Instrument errors, calibration errors, and representativeness errors were not taken into account during the model verification. This should also be kept in mind when evaluating model performance, because, for example, the estimate of a representativeness error (which is the greatest among the errors above) is close to 1 m s^{-1} for near-surface wind speed in a well-mixed boundary layer in complex terrain (e.g., Rife et al. 2004).

The statistical scores, such as the multiplicative mean systematic error (MBIAS, which is a ratio of mean modeled and observed wind speeds—MBIAS of unity implies no systematic error) and the root-mean-square error (RMSE; e.g., Wilks 2006) for the selected stations were calculated and averaged over monthly periods to show their seasonal variability (Figs. 3, 4). Mean annual values are shown in Table 1. For comparison with the ERA-40 dataset, the ALHR and DADA model output data were used with a 6-hourly frequency. The 1-hourly statistical scores for the ALHR and DADA models are given for reference in Table 1 and do not show notable differences.

For the continental station SLB (in weakly sloped terrain), annually averaged MBIAS shows a strong overestimation of ERA-40 wind speeds, with a yearly mean value of 1.51. The greatest systematic error is present in October (MBIAS = 2.59), which is the month with the weakest mean wind speed (0.82 m s^{-1}). The annual means of monthly systematic errors for ALHR (0.99) and DADA (1.01) data are significantly improved and are nearly negligible, although there does exist an intermonthly variability.

Among the coastal stations, ERA-40 performs the worst for station NOV, with an MBIAS of 0.69. Similar to the results for station SLB, the peak of increased MBIAS is present in October, which is again the month with the weakest mean wind speed (2.7 m s^{-1}). This issue is not a characteristic of ALHR and DADA data,

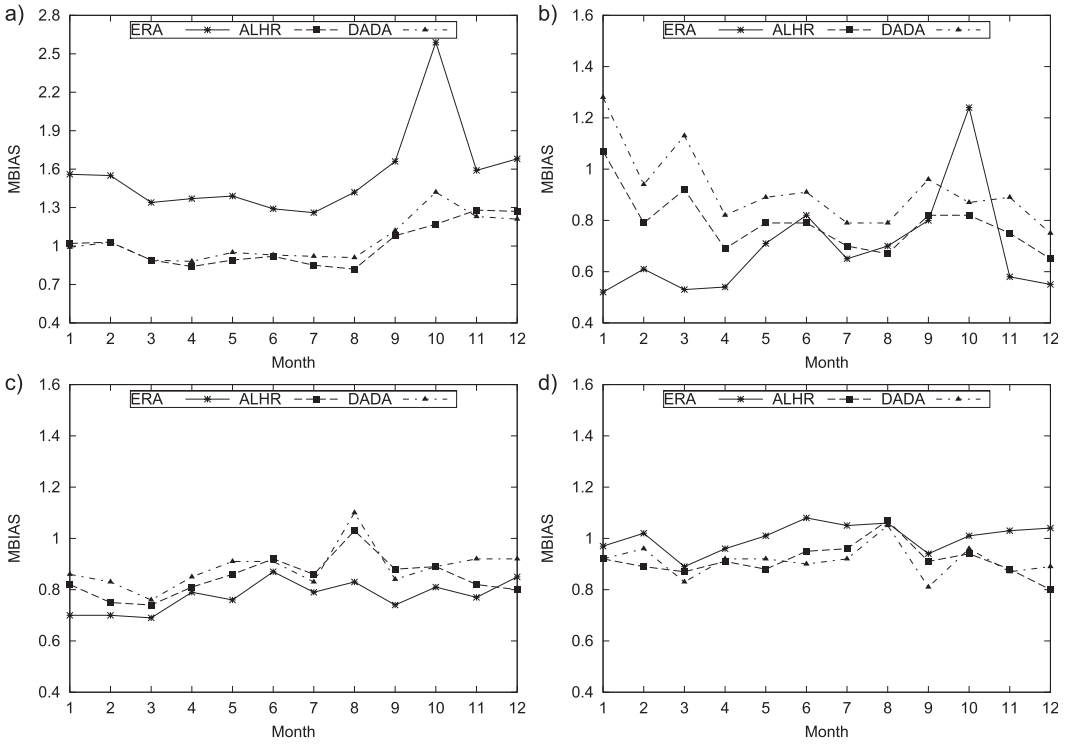

FIG. 3. Monthly variation of mean MBIAS (MBIAS = 1 is a perfect agreement) of modeled wind speed at 10 m AGL for stations (a) SLB, (b) NOV, (c) STM, and (d) DUB. Note the change in scale for station SLB.

suggesting that the overestimation might be due to a weaker ability of the ECMWF global model to simulate near-calm wind conditions. The mean annual MBIAS values for station NOV significantly improve for the ALHR and DADA data: 0.79 and 0.92, respectively. In a similar way, the MBIAS values for the station STM improve with higher grid spacing and are 0.78, 0.85, and 0.89 for ERA-40, ALHR, and DADA data, respectively, with no significant intermonthly variability. For the station DUB, however, the ERA-40 data show no systematic errors and outperform the ALHR and DADA models, which underestimate the mean wind speed by ~9%. This is likely to be at least partially related to the applied bilinear interpolation and to the fact that for this land station three out of four ERA-40 data grid points are located over the sea and are thus insufficiently representative of the actual station surroundings. At the DUB station, the intermonthly variability of MBIAS is the weakest among all of the analyzed stations.

Histograms of wind speed are shown in Fig. 5. The main characteristic of the wind speed distribution at station SLB is an underestimation of the frequency of weak winds in ERA-40 and a corresponding overestimation of the frequency of medium and stronger winds. This appears to be the main reason for the overall overestimation of mean wind speed in the global dataset, and it is probably related to the formulation of horizontal diffusion. On the other hand, at coastal sites the main feature is an underestimation of the frequency of stronger modeled wind speeds ($V > 6\ \mathrm{m\ s^{-1}}$) of all analyzed datasets that results in an overall underestimation of modeled mean wind speed. Again, with the exception of station DUB, dynamical downscaling improves the modeled frequencies of stronger winds speeds. Regardless of the weaker performance of mesoscale data at DUB stations, it is apparent that for stronger wind speeds, DADA data compare favorably to ALHR data for all analyzed stations. There are several factors that might contribute to the underestimation of stronger winds. These include model resolution and the resolution of the static lower boundary conditions, the appropriateness of physical parameterizations (especially the PBL scheme), the quality of lower boundary conditions, and the propagation of synoptic information through the coupling zone. Because of the importance of stronger winds for wind resource estimates in the region, the analysis of underlying factors (which is beyond the scope of the current paper) will play an important role in increasing the accuracy of future dynamical downscaling.

RMSE is smaller for the nearly flat terrain of continental Croatia than for the complex terrain of the eastern Adriatic coast. Thus, RMSE is the smallest for the station SLB, where the mean annual RMSE of the

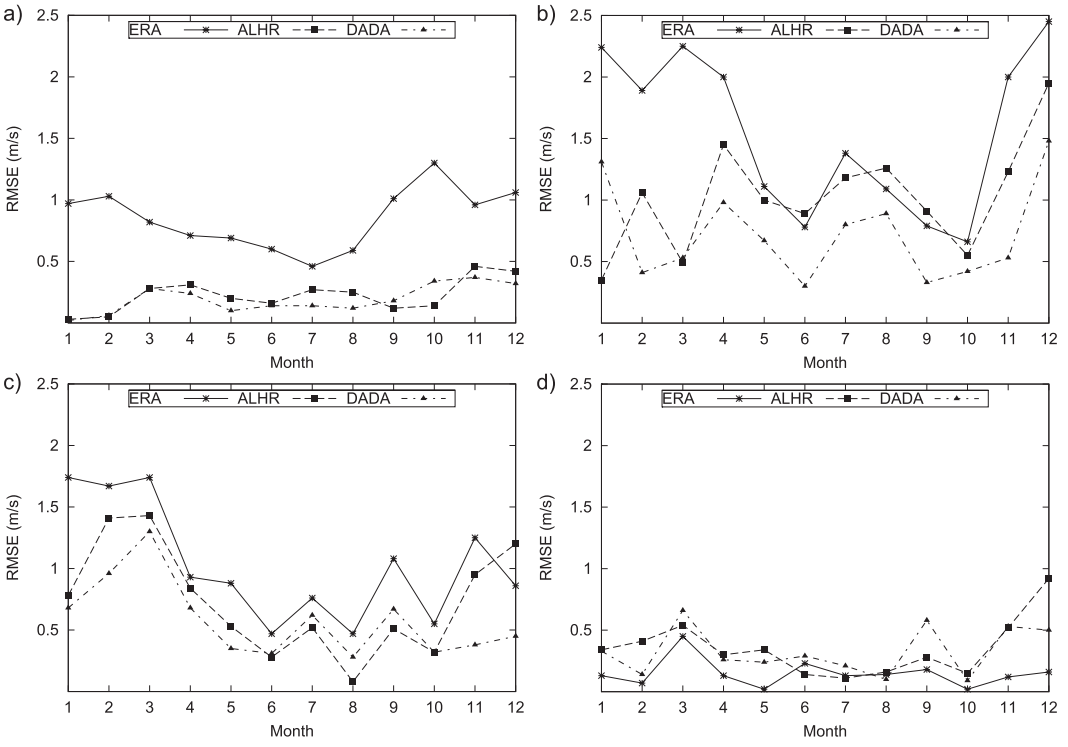

FIG. 4. Monthly variation of RMSE (m s^{-1}) at 10 m AGL for stations (a) SLB, (b) NOV, (c) STM, and (d) DUB. For easier comparison, RMSE was calculated with a 6-hourly frequency for all modeled data. For reference, average 1-hourly values are given in Table 1.

ERA-40 data (0.85 m s^{-1}) is strongly improved by dynamical downscaling and is equal to 0.22 m s^{-1} (ALHR) and 0.19 m s^{-1} (DADA). The least accurate results are for the station NOV, which is located exactly in the lee of the high and steep southern Velebit, and are equal to 1.55 (ERA-40), 1.03 (ALHR), and 0.73 (DADA) m s^{-1}. Because this station is located in the area where the bora is most directly associated with the wave-breaking regime, the low temporal predictability of this phenomenon and the resulting phase errors are most likely the main underlying reasons for the larger RMSE scores. Nevertheless, for stations NOV and STM, the systematic improvement in accuracy is evident as the RMSE of ERA-40 data are roughly halved in the DADA dataset. In contrast, RMSE scores for the DUB station suggest that the ALADIN model data at this station are outperformed by the ERA-40 data. Nevertheless, a slight increase in model accuracy is achieved with the use of the DADA when compared with the ALHR model. The highest intermonthly variability of RMSE is found for station NOV, followed by STM. The largest errors are found in the coldest part of the year and are characterized by a higher frequency of stronger winds in the area. Again, station DUB appears not to conform to the case of the two coastal stations farther to the north.

In general, statistical verification suggests that the dynamical downscaling results in more accurate wind climate estimates than does the global model reanalysis,

TABLE 1. Measured mean wind speed at 10 m AGL as well as MBIAS and RMSE as inferred from ERA-40 (ERA6), ALHR (AL6). and DADA (DA6) datasets with 6-hourly frequency during 2001 for stations SLB, NOV, STM, and DUB. A unit MBIAS (MBIAS = 1) points to a modeled dataset with no systematic error, whereas MBIAS of >1 (<1) indicates the overestimation (underestimation) of modeled data. For reference, 1-hourly values and statistics for ALHR and DADA datasets are given as well.

		MBIAS-6			RMSE-6				MBIAS-1		RMSE-1	
	Obs-6 (m s^{-1})	ERA6	AL6	DA6	ERA6	AL6	DA6	Obs-1 (m s^{-1})	AL1	DA1	AL1	DA1
SLB	1.74	1.51	0.99	1.01	0.85	0.22	0.19	1.72	0.99	0.99	0.21	0.21
NOV	4.26	0.69	0.79	0.92	1.55	1.03	0.73	4.32	0.78	0.91	1.04	0.71
STM	4.42	0.78	0.85	0.89	1.12	0.73	0.58	4.40	0.84	0.87	0.75	0.56
DUB	3.31	1.00	0.91	0.91	0.18	0.35	0.33	3.35	0.88	0.90	0.41	0.35

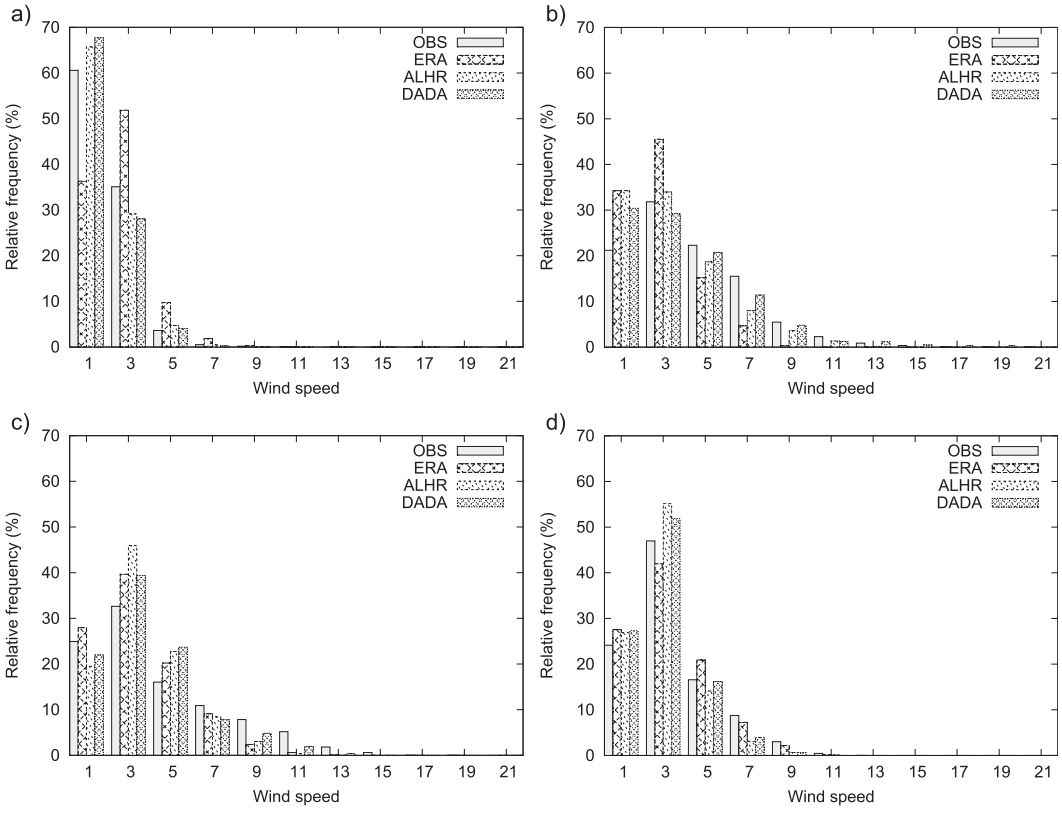

FIG. 5. Histograms of wind speed at 10 m AGL (bins of 2 m s^{-1}) for stations (a) SLB, (b) NOV, (c) STM, and (d) DUB.

with considerably smaller systematic and root-mean-square errors. The dynamical downscaling at 2-km grid spacing, carried out with a simplified and cost-effective model formulation, outperforms the results found for 8-km grid spacing. This systematic increase in mesoscale model accuracy is true in both the complex terrain of the eastern Adriatic coast and the nearly flat terrain of continental Croatia. While obviously the improvement of lower boundary conditions (e.g., representation of terrain and land use) that comes from increased horizontal resolution is the most important component of this benefit in complex terrain, we note that the nonlocal influence of an interaction between the atmosphere and complex terrain plays as well an important role for model accuracy in the surrounding flat terrain.

c. *Spectral analysis in the spatial domain*

It is known that the atmospheric kinetic energy spectrum of inherently 2D large-scale motions in the free troposphere follows a k^{-3} power law, where k is the wavenumber (e.g., Kraichnan 1967; Lilly 1969; Charney 1971; Boer and Shepherd 1983; Nastrom and Gage 1985). This shape shows great universality regardless of the latitude (midlatitudes), season, or altitude. A less steep $k^{-5/3}$ dependence on the smallest scales, typically not resolvable by mesoscale models, is associated with 3D cloud-resolving motions and turbulence scales (Kolmogorov theory). Between these scales, however, the mesoscale spectrum is not completely understood as the mesoscale motions are predominantly 2D but the kinetic energy spectrum is closer to $k^{-5/3}$ (e.g., Gage and Nastrom 1986; Lindborg 1999; Skamarock 2004). Nevertheless, spectral analysis in the spatial domain is an appealing tool for analysis of properties of mesoscale models on a variety of spatial scales and qualitative assessment of model performance.

Prior to calculations of kinetic energy, vorticity, and divergence spectra, a spatial subset of ERA-40 data was created to fit exactly the mesoscale model integration domain (which was 1920 km wide) with model levels interpolated to 37 levels of ALHR data. Spectra were calculated every 6 h (which is the availability of the ERA-40 reanalysis) for the entire year of 2001. The results of the dynamical adaptation were not used in this part of the evaluation because the domain used was too prohibitive in size to attempt comparison with the ERA-40 reanalysis.

The normalized kinetic energy spectrum is shown in Fig. 6a for both ERA-40 reanalysis and ALHR data at

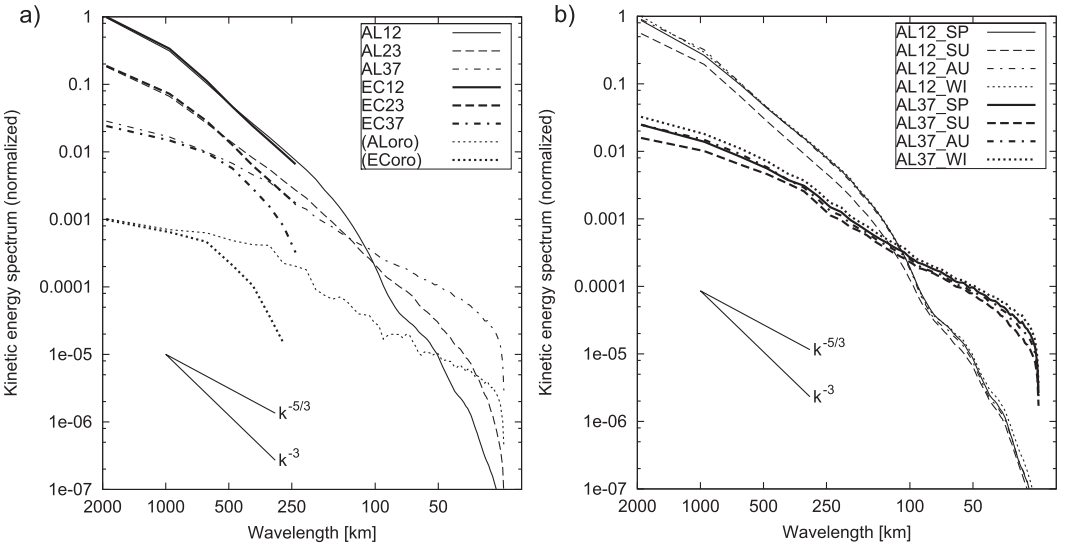

FIG. 6. Normalized kinetic energy spectra for ERA-40 (EC) and ALHR (AL) data at model levels (a) 12 (~300 hPa), 23 (~700 hPa), and 37 (~1000 hPa); and (b) its seasonal variability at model levels 12 (~300 hPa) and 37 (~1000 hPa). Orography spectra for ERA-40 (ECoro) and ALHR (ALoro) data (normalized and scaled by 0.001) are added to (a). Values beginning "1e" in this and subsequent figures indicate a value of 10 raised to the following characters (exponent).

model level 12 (~300 hPa), model level 23 (~700 hPa), and the lowest model level 37 (~1000 hPa). These levels correspond to the upper-, mid-, and near-surface troposphere. In addition, the orography energy spectrum (normalized and scaled by 0.001) is added to the figure for both ALHR and ERA-40 models. First, it is evident that the dynamical downscaling created a portion of mesoscale energy at scales below 250 km (thus unresolved by ERA-40 reanalysis). This part of the spectrum captures limited amounts of energy in the free atmosphere, but the kinetic energy of meso-β-scale (20–200 km) motions at near-surface levels is much greater than at the upper levels and indicates the importance of small-scale yet energetic processes near the surface.

In the upper troposphere and down to wavelengths of 250 km, ALADIN and ECMWF spectra are almost identical and conform to the k^{-3} law. At scales close to 300 km and lower, however, the spectrum of the ALADIN model does not show a gradual transition toward less steep behavior, suggesting that at these scales there is not enough mesoscale energy created near the tropopause. The underlying reason is not obvious, but it might be that model levels are too scarce near the tropopause (the vertical resolution at ~9 km MSL is close to 800 m) to account for mesoscale processes near the troposphere–stratosphere boundary (the intrusions and mesoscale portion of the upper-level jet dynamics). This model property was to some extent noticed in other studies of dynamical downscaling using the ALADIN model (e.g., Žagar et al. 2006), regardless of the chosen nesting ratio, domain size, or initial and boundary conditions.

In the midtroposphere (~700 hPa), the ERA-40 reanalysis shows less steep dependency than it does at upper levels. The ALADIN kinetic energy spectrum also deviates from the k^{-3} relationship and more closely resembles $\sim k^{-2}$ in the entire range of wavelengths that are unaffected by the diffusive end of the spectrum. A similar shape of the kinetic energy spectrum is found in the Weather Research and Forecasting mesoscale model (Skamarock 2004). The results at levels 12 and 23 (~300 and 700 hPa) suggest that the kinetic energy spectra at various altitudes in the free troposphere above complex terrain might be very different. Indeed, the shape of the kinetic energy spectrum at 700 hPa appears to be shifted toward the shape of the orography (and near-surface wind speed) spectrum. It seems that (although there is no relevant observed climatological data) this could be related to orographically induced, vertically propagating gravity waves over the complex terrain in the model domain (e.g., over the Alps, Apennines, and Dinaric Alps). Such gravity waves are a common phenomenon in the area and are very likely more often found in the midtroposphere than in the upper troposphere.

The flattening of the kinetic energy spectrum is even more obvious at near-surface levels where the spectrum is closer to $k^{-5/3}$. This illustrates the shape of the orography spectrum rather than properties of boundary layer turbulence that are characterized by three-dimensionality of motions since motions are not isotropic at scales resolved

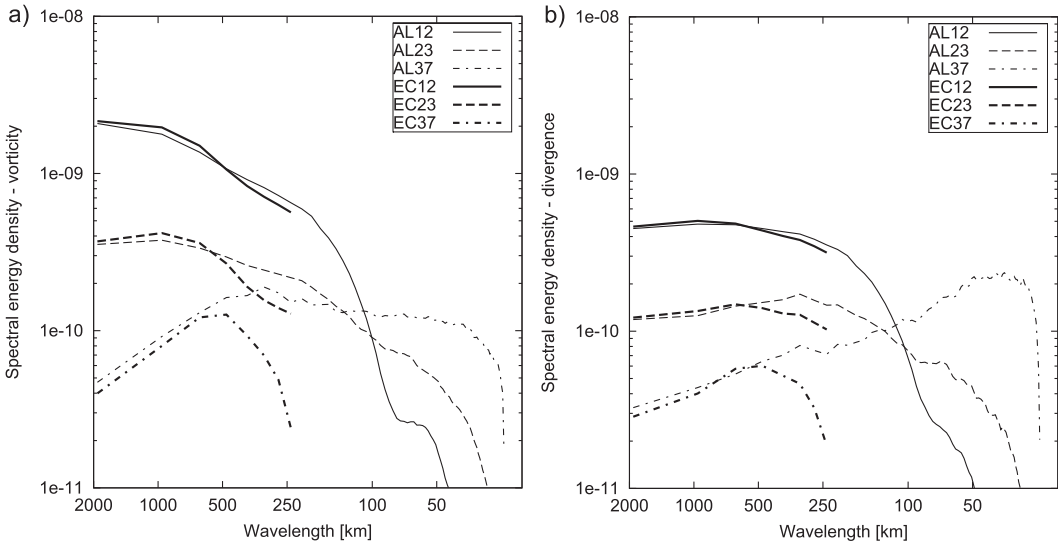

FIG. 7. Spectral energy density for ERA-40 (EC) and ALHR (AL) data at model levels 12 (~300 hPa), 23 (~700 hPa), and 37 (~1000 hPa) for (a) relative vorticity (b) divergence.

by the model. The resemblance of orography and near-surface spectra is almost complete and suggests that near-surface winds in the model are primarily adapted to orographic features. In contrast to the upper levels, progressively closer to the ground the kinetic energy spectra of the ALHR data and ERA-40 reanalysis diverge on increasingly larger scales. To study the effective model resolution, we study the deviation between the expected and modeled kinetic energy spectra at low wavelengths (e.g., Skamarock 2004). In our case, we consider k^{-3} at the upper levels and orography spectra at low levels as reference values. Near the surface, the ERA-40 spectrum begins to lose energy at scales of ~600 km, which is close to the $5dx$ of the ERA-40 grid spacing and is considerably larger than at the upper levels. On the other hand, the shape of ALHR spectra resembles the orographic one on scales down to and well below 50 km, which are scales much smaller than the corresponding ones at the upper levels. Thus, it appears that while the effective resolution of the ALADIN model improves when approaching the ground the opposite holds for the ERA-40 reanalysis. The underlying reasons for this are not obvious, but we note that, for the purpose of near-surface wind climate or resource estimates, the effective resolution plays an important role in determining the limits of the potential model performance.

Overall, the kinetic energy on scales over hundreds of kilometers is much stronger at the upper levels than it is near the surface, regardless of the model. In contrast, at scales of slightly over 100 km and less the kinetic energy of near-surface motions becomes dominant. This clearly implies that high-resolution mesoscale dynamical downscaling, which aims to study near-surface regional wind climate or resources, needs to be highly reliable at scales sufficiently small to account for the considerate amount of energy contained in the near-surface meso-β scales of motion.

The seasonal dependency of the kinetic energy spectrum of the ALADIN model is shown in Fig. 6b. Regardless of the level, the greatest amount of kinetic energy is found during the winter, followed by spring and autumn. There is somewhat less kinetic energy during the summer than during the rest of the year. This reflects the weaker upper-level dynamics, as well as the lower near-surface wind speeds, in the region during the warmest season of the year. In accordance with the observational evidence mentioned above, spectra at different levels have similar shapes regardless of the season.

Spectral energy densities of vorticity and divergence at the upper troposphere (model level 12; ~300 hPa), midtroposphere (model level 23; ~700 hPa), and lower troposphere (model level 37; ~1000 hPa) are shown in Figs. 7a,b. The ALADIN output and ERA-40 reanalysis compare well for larger scales roughly down to 600 km. Below this level, the divergence and vorticity from the ERA-40 dataset begin to progressively lose energy as they become closer to the surface, confirming the kinetic energy spectrum considerations.

As anticipated, the vorticity field is more energetic than the divergence at larger scales. At wavelengths slightly over 100 km and less, however, divergence at the upper and middle levels begins to be almost as energetic as vorticity. Furthermore, at these scales, divergent motions are even more energetic near the surface than they

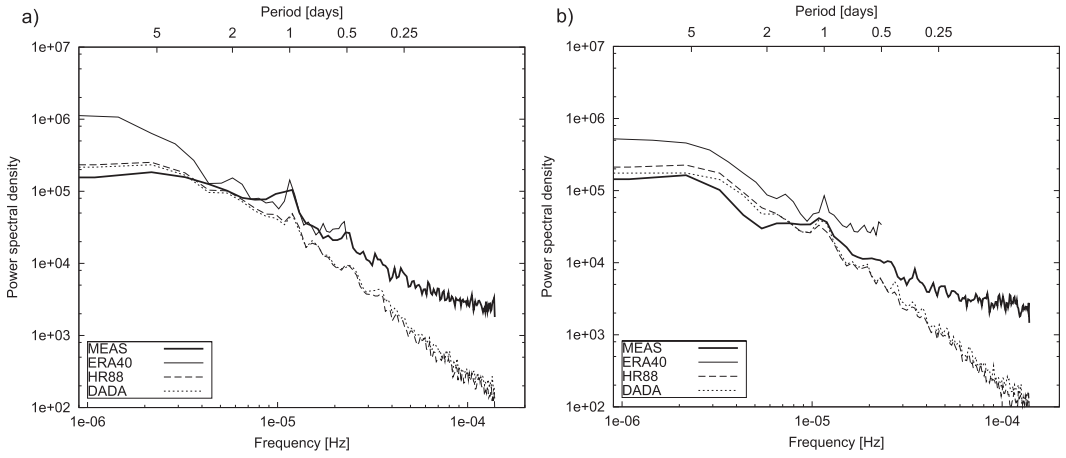

FIG. 8. Power spectra of 10-m (a) zonal and (b) meridional wind components of measured and modeled ERA-40, ALHR, and DADA data for station SLB.

are aloft. As such, the near-surface divergence becomes several times more energetic than vorticity at the same level, suggesting that surface forcing results in the creation of unbalanced divergent (rather than balanced rotational) meso-β-scale motions. Therefore, the importance of near-surface divergence illustrates a potential constraint of mass-consistent nondivergent models in simulating the near-surface wind climates over complex terrain.

d. Spectral analysis in the temporal domain

Because several measurement stations are located in the proximity of both complex terrain and the seashore and are characterized by motions at different temporal scales, the success of the analyzed models was verified against the measured data using spectral verification in the temporal domain. Because typical diurnal rotation of winds in the Adriatic (Telišman Prtenjak and Grisogono 2007) partially hides the diurnal spectral peak if spectral analysis is performed using wind speed values, spectral verification was achieved through the comparison of spectral power density functions of both of the horizontal wind components, u and v. In the case of continental station SLB, u and v correspond to zonal and meridional directions. In the case of coastal stations, the coordinate system is rotated such that u and v correspond to cross- and along-mountain directions (corresponding to the main axes of the Dinaric Alps). Prior to spectral decomposition achieved using the Welch (1967) method, data were detrended (data were divided into ~10-day segments and the best linear fit was removed). A few missing data were provided using regression analysis. It should be kept in mind that spectra were calculated for ERA-40 data with 6-hourly frequency and for other datasets using 1-hourly temporal resolution. We note that 6 h is the maximal temporal resolution of the ERA-40 output and that differences in statistical verification were minor, however (see Table 1).

Power spectral density functions for both zonal and meridional wind components for station SLB are shown in Figs. 8a,b. The largest portion of the measured spectrum is associated with synoptic and mesoscale motions. These larger-than-diurnal scales of motion (here defined as motions of periods of >26 h) are more energetic for the zonal wind component and are likely associated primarily with the predominantly westerly zonal flow and the more complex terrain found in meridional directions. In the ERA-40 data, the energy of these motions is greatly overestimated, especially for the meridional wind component. In the ALADIN model data, however, larger-than-diurnal circulations are simulated well. The overestimation of this larger-scale energy associated with meridional wind directions in ERA-40 is likely due to the nonlocal influence of the Dinaric Alps to the south/southwest of the station, which are not fully resolved in the reanalysis data. That is, because the Dinaric Alps partially block the southwesterly sirocco winds and channel them in the southeasterly direction over the Adriatic Sea, an unresolved mountain range could contribute to overestimation of these winds over the inland area. The secondary diurnal maximum, which is underestimated in both the ALHR and DADA simulations, is more accurately described by the ERA-40 data, however. Although there are no clear indications as to the underlying reasons why these diurnal circulations are not sufficiently energetic in the ALHR simulations, it is clear that, because of the gentle slope of the surrounding terrain, the DADA model does not have much potential to improve this deficiency. The prominent underestimation of the power

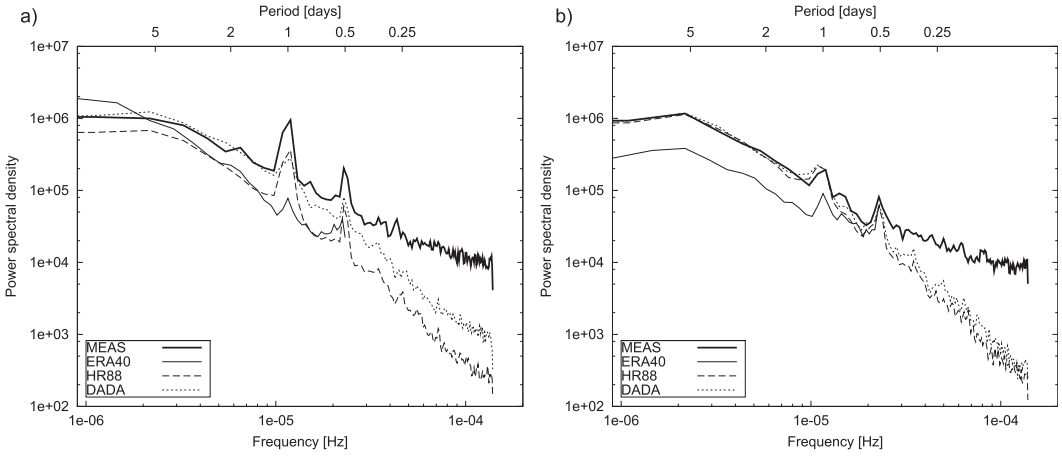

FIG. 9. Power spectra of 10-m (a) cross-mountain and (b) along-mountain wind components (corresponding to the main axes of the Dinaric Alps) of measured and modeled ERA-40, ALHR, and DADA data for station NOV.

spectral density functions in the temporal range of less than 12 h appears to hold for all stations and will be discussed later in the text.

The results of the spectral decomposition for the coastal stations are shown in Figs. 9a,b, 10a,b, and 11a,b. A mentioned earlier, the u and v components for the coastal stations are rotated and correspond to cross- and along-mountain directions. The spectral power over the whole frequency range at the coastal stations is overall much higher than it is for the SLB station. Among all of the coastal stations, the ALADIN model data show the greatest accuracy for the NOV station regardless of the underestimation of the power of diurnal motions. The considerable improvement in comparison with the global reanalysis is apparent for all frequency ranges and especially for the DADA results. The improvement of the DADA model is evident for the cross-mountain direction only, because the results for the along-mountain direction are nearly identical to observations for both ALHR and DADA data. For the STM station, the ERA-40 model data simulate the power of synoptic motions (periods over a few days) reasonably well but underestimate the larger-than-diurnal part of the mesoscale range. On the other hand, the ALHR and DADA data better simulate the overall shape of larger-than-diurnal periods of motions but generally underestimate the synoptic part of the measured power spectrum. For the power of larger-than-diurnal motions, the DADA results are improved for the cross-mountain direction but are less accurate for the along-mountain direction. The results of downscaling are far better in the diurnal range: for the mostly cross-mountain diurnal circulations present at this station the ALHR and DADA models considerably outperform the

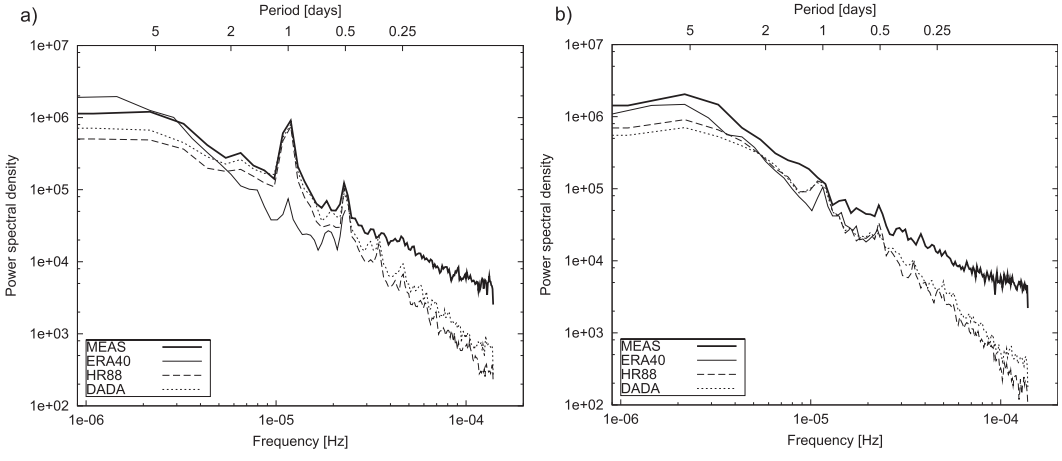

FIG. 10. As in Fig. 9, but for station STM.

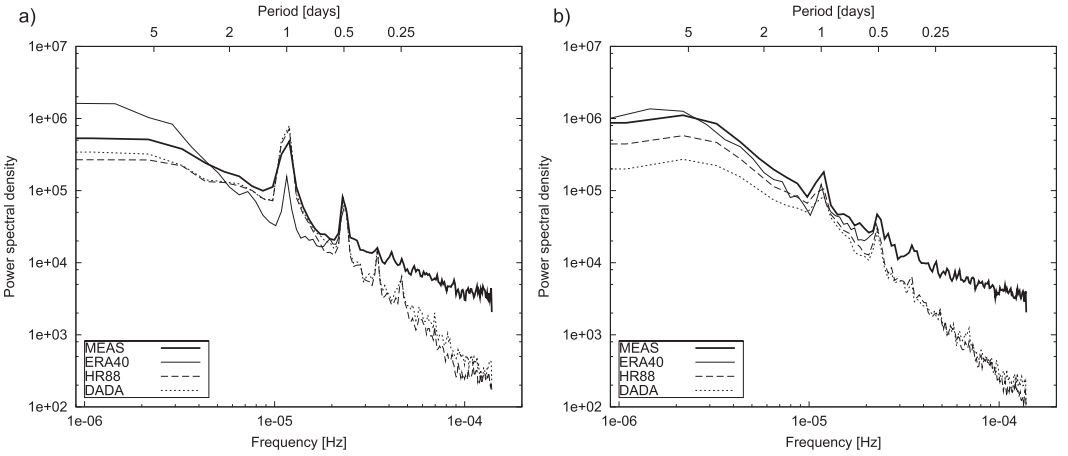

FIG. 11. As in Fig. 9, but for station DUB.

ERA-40 data. This is likely to be the main added value of downscaling at this station. For station DUB, the ERA-40 results are more accurate than those of the ALADIN model data for the larger-than-diurnal portion of the along-mountain wind component spectrum; in the ALHR and DADA data the power of larger-than-diurnal circulations is underestimated. In the cross-mountain direction, the ALADIN model data are still underestimated but show far more accurate shapes than in the ERA-40 data. The main benefit of the mesoscale datasets for this station as well appears to be the well-simulated strength of the cross-mountain diurnal circulations.

Thus, for all of the coastal stations, the power spectra of the wind speed for the DADA data (relative to the ALHR data) are improved for the cross-mountain component. With the exception of the NOV station, where both the ALHR and DADA spectra are equal to the observed one, spectra of the DADA data for coastal stations are less accurate than for the ALHR data for the along-mountain wind component, however. Apart from the potential changes in wind direction introduced by the higher-resolution lower boundary conditions in the DADA model, this may also be related to the properties of the prevalent cross-mountain bora and the along-mountain jugo winds. That is, it is known that the response of the bora downslope low-level jet along the eastern Adriatic coast (in the lee of the Dinaric Alps) is almost entirely proportional to the cross-mountain pressure gradient (e.g., Horvath and Ivančan-Picek 2008) and is therefore well suited for dynamical adaptation (see the introduction). On the other hand, along-mountain winds (e.g., the jugo winds) are much less influenced by pressure perturbation induced by the Dinaric Alps. Therefore, the results suggest that the primary application of dynamical adaptation is likely related to better simulations of cross-mountain bora-type flows. On the other hand, because of mixed results for the along-mountain wind component, the performance of dynamical adaptation for other wind systems in the region and for wind climates not primarily related to bora-type flows remains to be analyzed further in more detail.

Unlike the SLB station, all of the coastal stations show the existence of a tertiary maximum that is presumably associated with land–sea breeze circulation. These motions of semidiurnal periods (11–13 h) are reproduced very accurately in the ALADIN model, especially for the cross-mountain direction (a comparison with the ERA-40 data is not fully applicable since 12 h corresponds to the time period of the Nyquist[5] frequency for the ERA-40 data). Last, a common feature of the ALADIN model simulations appears to be the underestimation of the spectral power of subsemidiurnal motions. Similar results were achieved for dynamical downscaling with the ALADIN model over the complex terrain of Slovenia, regardless of the domain size and nesting strategy (Žagar et al. 2006). This suggests that the ability of the ALADIN model to reproduce mesoscale energy on less-than-semidiurnal temporal scales is limited in the current model setup. Given the generous spinup time (12 h), it is more likely that the low spatial and temporal predictability of motions at less-than-semidiurnal scales, and possibly the too-strong numerical diffusion in the ALADIN model, are the main contributors to this underestimation. Therefore, although it is not particularly relevant for the Croatian region, the lack of energy in motions with temporal scales of less

[5] Nyquist frequency is one-half times the sampling frequency of a discrete-sampling signal-processing system.

than 12 h might constrain the use of the current version of the ALADIN mesoscale model for areas where a considerable part of the spectral power exists on the subsemidiurnal part of the spectrum.

4. Conclusions

To assess the climatological basis for wind energy resource assessments, dynamical downscaling was performed for the wider Croatian region, part of which is prone to downslope bora windstorms. Downscaling was carried out with the ALADIN model driven by the ERA-40 reanalysis data for a 10-year period. The modeling system was initiated daily in two subsequent steps: 1) the full ALADIN model integration (ALHR) to 8-km horizontal grid spacing with a 60-min output frequency and 2) the simplified ALADIN model version, so-called dynamical adaptation (DADA) initiated by the ALHR model to 2-km horizontal grid spacing. The model evaluation was performed for the wind speed variable, and all model data were evaluated against the measured data using both statistical and spectral verification.

Results suggest that wind resources are considerably greater in the coastal part than in the continental part of Croatia. The near-surface mean wind speed is highest in areas of the Vratnik Pass and downstream of it, on the lee sides of Velebit Mountain, and on prominent mountaintops. While mountaintops are frequent regions of enhanced wind resources, the other areas mentioned are known for bora severity and frequency, clearly identifying the primary role of bora in determining the wind climate of the wider area of the eastern Adriatic.

Statistical verification (performed with the use of multiplicative bias and root-mean-square error), suggests that the downscaling was very successful. In general (with the exception of the DUB station), the accuracy of the ALHR model values increased relative to those of ERA-40, both in flat and complex coastal terrain. Furthermore, the added value of the DADA in comparison with the ALHR model results is notable for all stations analyzed. The final downscaling results produced with dynamical adaptation with a 2-km horizontal grid spacing show higher accuracy for continental Croatia and the SLB station (where systematic error is 1%) than for coastal complex terrain and the NOV, STM, and DUB stations (where the mean wind speed value is on average underestimated by close to 10%). The underestimation at coastal stations is due to underestimation of the frequency of stronger wind speeds. Nevertheless, the distribution of stronger winds modeled with DADA compares favorably to both ERA-40 and ALHR data. RMSE values scaled with the observed mean wind speeds are similar among the analyzed stations and are close to 12% of mean wind speed value.

The scale-dependent evaluation, performed with the use of spectral analyses in both spatial and temporal domains, allowed for model assessment on a variety of scales. Kinetic energy spectra compare well to theoretical and observational evidence gathered at the midlatitudes, and its shapes show no dependence on season. In the upper troposphere (~300 hPa) and for scales over several hundreds of kilometers, the kinetic energy spectra acquire k^{-3} dependency for both ERA-40 and ALADIN model results. In the midtroposphere (~700 hPa), the spectrum relaxes to nearly k^{-2}, and near the surface it closely resembles the shape of orography spectra (roughly $k^{-5/3}$), illustrating the effect of adaptation of near-surface winds to model orography. The differences in spectra at mid- and upper levels suggest that orographically induced vertically propagating gravity waves likely play a considerable role in determining the shape of the kinetic energy spectra in the free atmosphere over complex terrain. In the shared portion of the wavelength domain, the differences between ERA-40 and ALADIN data are nonexistent for larger wavelengths. At scales below ~700 km, however, ERA-40 has progressively larger energy deficit the closer to the ground. On the other hand, a major flaw of the ALADIN model kinetic energy spectrum seems to be an unfavorable steepening of the k^{-3} dependency at upper levels only and on scales below a few hundred kilometers. At the lower levels, the ALADIN model spectrum resembles the orography spectrum down to scales well below 50 km. Thus, the effective model resolution is vertically dependent in both ERA-40 and ALHR data.

As expected, vorticity is more energetic than divergence at the upper levels, especially at larger scales. Near the surface and for scales slightly above 100 km and less, however, the divergence spectrum is several times as intensive as the vorticity spectrum. Thus, mesoscale simulations contain a considerable amount of energy on meso-β scales (20–200 km) related to near-surface unbalanced divergent motions. This illustrates an inherent constraint of mass-consistent nondivergent models for assessing near-surface wind climatology or resource estimates.

Spectral decomposition of measured and modeled data in the temporal domain shows reasonable accuracy over the different temporal scales of motion for all of the model datasets, with a little difference between the ALHR and DADA spectra. For continental Croatia, downscaling improves the global model spectrum primarily in the larger-than-diurnal scales of motion; this is probably due to the nonlocal influence of the orography of the Dinaric Alps to the south. The downscaled diurnal

motions are not as accurate as those of the ERA-40 reanalysis, however. At the coastal stations, the accuracy of the modeled power spectrum varies and the results show somewhat underestimated values in the synoptic and mesoscale ranges. The main benefits of dynamical downscaling are evident for frequency distributions of stronger winds (especially at the station with the strongest wind speeds, NOV) and generally for all of the coastal stations in the diurnal frequency range. Relative to the ALHR data, the DADA power spectra are improved for the cross-mountain (with respect to the orientation of Dinaric Alps) wind component at all stations; this is in large part related to the better simulations of bora flows. On the other hand, mixed results are achieved for the along-mountain wind component. This might be related to the induced changes in wind direction; further assessment of the potential benefits and limitations of DADA for applicability in wind climates not governed by bora-type flows remains to be investigated. Although the tertiary semidiurnal maxima (not available from the ERA-40 reanalysis) are well simulated in mesoscale datasets, the spectral power of motions with less-than-semidiurnal periods is strongly underestimated. Although the portion of power in this frequency range is almost negligible for the analyzed stations in Croatia, this model feature might constrain use of the model in areas with considerable amounts of energy present at these scales.

The importance of strong mesoscale local winds (such as the bora and jugo) for wind climate and resource estimates in the coastal and complex terrains of Croatia, and the remaining uncertainties in numerical modeling of these phenomena, confirm the need for further improvement of the results of dynamical downscaling and wind resource estimates for the region. Simplified dynamical adaptation proves a useful and cost-effective alternative at scales of a few kilometers, but the added value comes mostly from the increased horizontal resolution of the orography and land use. In terms of wind climate or resource estimates, however, there is limited knowledge on the disadvantages of the reduced complexity of dynamical adaptation in comparison with the full-physics model-formulation results. It is likely that more detailed dynamical downscaling of wind climate and resources would require the use of nonsimplified meteorological models on subkilometer horizontal grid spacing. With regard to the worldwide appearance of bora-type flows, analysis and numerical simulations of bora gustiness and turbulence do remain major research challenges related to both meteorological and wind energy applications in complex terrain.

Acknowledgments. This study was supported by HEP-OIE d.o.o, UKF Grant 16/08 through the WINDEX project (www.windex.hr) and the Project 004-1193086-3036 funded by the Ministry of Science, Technology and Sports of Croatia. The authors are grateful to Melita Perčec-Tadić for her assistance with the graphical presentation of the mean wind speed map. We appreciate the suggestions and comments of two anonymous reviewers that considerably improved the paper.

REFERENCES

Bajić, A., 1989: Severe bora on the northern Adriatic. Part I: Statistical analysis. *Rasprave-Pap.,* **24,** 1–9.

Beck, A., B. Ahrens, and K. Stadlbacker, 2004: Impact of nesting strategies in dynamical downscaling of reanalysis data. *Geophys. Res. Lett.,* **31,** L19101, doi:10.1029/2004GL020115.

Belušić, D., and Z. B. Klaić, 2006: Mesoscale dynamics, structure and predictability of a severe Adriatic bora case. *Meteor. Z.,* **15,** 157–168.

Boer, G. J., and T. G. Shepherd, 1983: Large-scale two-dimensional turbulence in the atmosphere. *J. Atmos. Sci.,* **40,** 164–184.

Bubnova, R., G. Hello, P. Benard, and J. F. Geleyn, 1995: Integration of fully elastic equations cast in the hydrostatic pressure terrain-following coordinate in the framework of ARPEGE/ALADIN NWP system. *Mon. Wea. Rev.,* **123,** 515–535.

Cavaleri, I., L. Bertotti, and N. Tescaro, 1997: The modelled wind climatology of the Adriatic Sea. *Theor. Appl. Climatol.,* **56,** 231–254.

Charney, J. G., 1971: Geostrophic turbulence. *J. Atmos. Sci.,* **28,** 1087–1095.

Davies, H. C., 1976: A lateral boundary formulation for multi-level prediction models. *Quart. J. Roy. Meteor. Soc.,* **102,** 405–418.

Gage, K. S., and G. D. Nastrom, 1986: Theoretical interpretation of atmospheric wavenumber spectra of wind and temperature observed by commercial aircraft during GASP. *J. Atmos. Sci.,* **43,** 729–740.

Geleyn, J. F., 1987: Use of a modified Richardson number for parametrizing the effect of shallow convection. *J. Meteor. Soc. Japan,* (Special NWP Symp. Vol.), 141–149.

——, and A. Hollingsworth, 1979: An economical analytical method for computation of the interaction between scattering and line absorption of radiation. *Contrib. Atmos. Phys.,* **52,** 1–16.

——, C. Girard, and J.-F. Louis, 1982: A simple parametrization of moist convection for large-scale atmospheric models. *Beitr. Phys. Atmos.,* **55,** 325–334.

Giard, D., and E. Bazile, 2000: Implementation of a new assimilation scheme for soil and surface variables in a global NWP model. *Mon. Wea. Rev.,* **128,** 997–1015.

Göhm, A., G. J. Mayr, A. Fix, and A. Giez, 2008: On the onset of bora and the formation of rotors and jumps near a mountain gap. *Quart. J. Roy. Meteor. Soc.,* **134,** 21–46.

Grisogono, B., and D. Belušić, 2009: A review of recent advances in understanding the meso- and microscale properties of the severe Bora wind. *Tellus,* **61A,** 1–16.

Horvath, K., and B. Ivančan-Picek, 2008: A numerical analysis of a deep Mediterranean lee cyclone: Sensitivity to mesoscale potential vorticity anomalies. *Meteor. Atmos. Phys.,* **113,** 161–171.

——, Y.-L. Lin, and B. Ivančan-Picek, 2008: Classification of cyclone tracks over Apennines and the Adriatic Sea. *Mon. Wea. Rev.,* **136,** 2210–2227.

——, S. Ivatek-Šahdan, B. Ivančan-Picek, and V. Grubišić, 2009: Evolution and structure of two severe cyclonic bora events:

Contrast between the northern and southern Adriatic. *Wea. Forecasting,* **24,** 946–964.

Ivatek-Šahdan, S., and M. Tudor, 2004: Use of high-resolution dynamical adaptation in operational suite and research impact studies. *Meteor. Z.,* **13,** 99–108.

Jurčec, V., B. Ivančan-Picek, V. Tutiš, and V. Vukičević, 1996: Severe Adriatic jugo wind. *Meteor. Z.,* **5,** 67–75.

Kållberg, P., A. Simmons, S. Uppala, and M. Fuentes, 2004: The ERA-40 archive. ECMWF ERA-40 Project Rep. Series, 17, 1–35.

Kessler, E., 1969: *On the Distribution and Continuity of Water Substance in Atmospheric Circulations*. *Meteor. Monogr.,* No. 10, Amer. Meteor. Soc., 84 pp.

Klemp, J. B., and D. R. Durran, 1987: Numerical modelling of bora winds. *Meteor. Atmos. Phys.,* **36,** 215–227.

Kraichnan, R. H., 1967: Inertial ranges in two-dimensional turbulence. *Phys. Fluids,* **10,** 1417–1423.

Lilly, D. K., 1969: Numerical simulation of two-dimensional turbulence. *Phys. Fluids,* **12** (Suppl. II), 240–249.

Lindborg, E., 1999: Can the atmospheric kinetic energy spectrum be explained by two-dimensional turbulence? *J. Fluid Mech.,* **388,** 259–288.

Louis, J.-F., M. Tiedke, and J. F. Geleyn, 1982: A short history of PBL parametrization at ECMWF. *Proc. ECMWF Workshop on Planetary Boundary Layer Parameterization,* Reading, United Kingdom, ECMWF, 59–79.

Lynch, P., and X. Y. Huang, 1994: Diabatic initialization using recursive filters. *Tellus,* **46A,** 583–597.

Machenhauer, B., and J. E. Haugen, 1987: Test of spectral limited area shallow water model with time-dependent lateral boundary conditions and combined normal mode/semi-Lagrangiean time integration schemes. *Proc. ECMWF Workshop: Techniques for Horizontal Discretization in Numerical Weather Prediction Models,* Reading, United Kingdom, ECMWF, 361–377.

Makjanić, B., 1976: A short account of the climate of the town Senj. *Local Wind Bora,* M. M. Yoshino, Ed., University of Tokyo Press, 145–152.

Mass, C. F., D. Ovens, K. Westrick, and B. A. Colle, 2002: Does increasing horizontal resolution produce more skillful forecasts? *Bull. Amer. Meteor. Soc.,* **83,** 407–430.

Nastrom, G. D., and K. S. Gage, 1985: A climatology of atmospheric wavenumber spectra of wind and temperature observed by commercial aircraft. *J. Atmos. Sci.,* **42,** 950–960.

Poje, D., 1992: Wind persistence in Croatia. *Int. J. Climatol.,* **12,** 569–582.

Rife, D. L., C. A. Davis, and Y. Liu, 2004: Predictability of low-level winds by mesoscale meteorological models. *Mon. Wea. Rev.,* **132,** 2553–2569.

Ritter, B., and J. F. Geleyn, 1992: A comprehensive radiation scheme for numerical weather prediction models with potential applications in climate simulations. *Mon. Wea. Rev.,* **120,** 303–325.

Simmons, A. J., and D. M. Burridge, 1981: An energy and angular momentum conserving vertical finite-difference scheme and hybrid vertical coordinate. *Mon. Wea. Rev.,* **109,** 758–766.

Skamarock, W. C., 2004: Evaluating mesoscale NWP models using kinetic energy spectra. *Mon. Wea. Rev.,* **132,** 3019–3032.

Smith, R. B., 1985: On severe downslope winds. *J. Atmos. Sci.,* **42,** 2597–2603.

——, 1987: Aerial observations of the Yugoslavian bora. *J. Atmos. Sci.,* **44,** 269–297.

Telišman Prtenjak, M., and B. Grisogono, 2007: Sea/land breeze climatological characteristics along the northern Croatian Adriatic coast. *Theor. Appl. Climatol.,* **90,** 201–215.

Troen, I., and E. L. Petersen, 1989: *European Wind Atlas*. Risø National Laboratory, 656 pp.

Welch, P. D., 1967: The use of fast Fourier transform for the estimation of power spectra: A method based on time averaging over short, modified periodograms. *IEEE Trans. Audio Electroacoust.,* **AU-15** (6), 70–73.

Wilks, D. S., 2006: *Statistical Methods in the Atmospheric Sciences*. 2nd ed. International Geophysics Series, Vol. 59, Academic Press, 627 pp.

Yoshino, M. M., 1976: *Local Wind Bora*. University of Tokyo Press, 289 pp.

Žagar, M., and J. Rakovec, 1999: Small-scale surface wind prediction using dynamic adaptation. *Tellus,* **51A,** 489–504.

Žagar, N., M. Žagar, J. Cedilnik, G. Gregorič, and J. Rakovec, 2006: Validation of mesoscale low-level winds obtained by dynamical downscaling of ERA-40 over complex terrain. *Tellus,* **58A,** 445–455.

Zaninović, K., and Coauthors, 2008: *Klimatski Atlas Hrvatske 1961–1990, 1971–2000 (Climate Atlas of Croatia 1961–1990, 1971–2000)*. Meteorological and Hydrological Service, 200 pp.